Single-Shot Fourier-Slice Dual-Comb Spectroscopy

Bachana Lomsadze*, Skyler Weight, and Peyton Clark

***Abstract*—Multidimensional coherent spectroscopy is a powerful method for studying materials' optical properties. It also has potential to be used for chemical sensing applications as it allows the measurements of samples' energy level structures as well as couplings between the excited states resonances. This coupling information is the key to identify whether or not the sample contains a mixture of analytes. Coupling information is not easily accessible using one-dimensional linear or nonlinear methods, necessitating more complex multidimensional experimental techniques. However, multidimensional techniques require bulky apparatus, complex stabilization schemes, and/or long acquisition times that prevent them from being used outside the lab. Here we propose and demonstrate a new and simple approach that enables the measurements of the main absorption lines as well as the couplings between the excited states resonances extremely fast (tens to hundreds of μs) without measuring the full multidimensional spectra. This approach is based on the Fourier-slice theorem and was inspired by frequency comb technology, particularly dual-comb spectroscopy. Our approach uses free-running lasers and co-linear geometry, and with the development of compact lasers this approach can become field-deployable for sensing applications. We demonstrate the concept on rubidium vapor.**

***Index Terms*—Dual comb spectroscopy, multidimensional coherent spectroscopy, Photon echo, Fourier-slice theorem.**

I. Introduction

Optical spectroscopy is a powerful tool for fundamental science as it allows the measurements of the energy structures and optical properties of a wide range of materials. In addition, optical spectroscopy is widely used for many practical applications such as chemical identification, medical imaging, etc. Over the years, linear and nonlinear techniques such as Fourier Transform (FTIR) spectroscopy [1], fluorescence spectroscopy, coherent anti-stokes Raman spectroscopy (CARS) [2], [3], etc have proven to be very powerful for these applications [4]. When using these methods, sample identification process is usually performed by measuring spectra (e.g. linear absorption or CARS) of the sample of interest and then comparing them to the databases of known spectra. However, these techniques are one-dimensional and they have significant limitations especially when probing heterogeneous samples with spectrally overlapped lines. To put it simply, they face challenges to distinguish between a three-level system with two resonant frequencies f_1 and f_2 (energy level diagram shown in figure 1 (c) at the top), a mixture of two independent two-level systems with the same frequencies (shown in figure 1 (d) at the top), and a mixture of coupled two independent two-level systems with the same frequencies (shown in figure 1 (e) at the top). Obviously, one-dimensional spectra of these systems would look identical which is a critical limitation for chemical sensing applications especially when probing samples with complex energy structures and without prior knowledge of its constituent analytes.

These limitations are typically overcome by using multidimensional methods e.g. multidimensional coherent spectroscopy (MDCS) [5]. Detailed description of different approaches for MDCS can be seen elsewhere [5], [6], [7] but here we briefly describe one of the most commonly used approaches. This approach uses a sequence of three pulses (A* - complex phase conjugated, B, C) as shown in figure 1 (a) incident on the sample of interest and generates a four-wave mixing (FWM) signal which is then heterodyne detected, using a local oscillator pulse, as a function of the delays between the excitation pulses. The recorded time domain interferogram (figure 1 (b)) is then Fourier transformed with respect to the time delays between the incident pulses and over the time period during which the signal is emitted (t and τ) to generate a multidimensional coherent spectrum (e.g. figure 1 (c)). We should note that the (A*, B, C) excitation scheme is also referred to as a rephasing or photon echo sequence [8]. In this sequence, A* pulse creates a coherence between ground ($|g\rangle$) and excited ($|e\rangle$) states. This coherence then evolves during τ shown in figure 1 (a) (blue trace). Pulse B then converts the coherence into the population state and then the same pulse (C) converts it to the third order coherence which emits a FWM signal during t (blue trace). The evolution and emission processes evolve with opposite phases and for an inhomogeneously broadened system this causes the excited state resonances to rephase, interfere constructively at t=τ, and create a photon echo signal (red).

This excitation scheme has many advantages and among them is the ability to measure the couplings between the excited states. This point is demonstrated in figures 1 (c, d, e) where cartoons of 2D spectra are plotted for the corresponding systems shown at the top. On the 2D spectra, diagonal peaks (along the white dotted line) correspond to samples' resonances and off diagonal peaks determine the cross peaks indicating that the resonances belong to the same system (figures 1 (c)) or two independent systems are coupled to each other (figures 1 (e)).

Clearly, MDCS provides critical information for chemical sensing and imaging applications which is not easily accessible using traditional 1D methods. However, MDCS experimental setups either utilize bulky and slow mechanical moving stages and complex phase cycling schemes [9], [10], [11], [12], [13], or multiple asynchronously scanning lasers [14] and complex locking electronics [15], [16].

In this paper we propose a simpler approach that enables rapid measurements of the main as well as the coupling peaks (cross peaks) without measuring the full multidimensional

B. Lomsadze is an Associate Professor of Physics (e-mail: blomsadze@scu.edu). B. Lomsadze, S. Weight, P. Clark are with the Department of Physics, Santa Clara University, 500 El Camino Real, Santa Clara, CA, 95053.

This article has been accepted for publication in IEEE Photonics Technology Letters. This is the author's version which has not been fully edited and content may change prior to final publication. Citation information: DOI 10.1109/LPT.2023.3325799

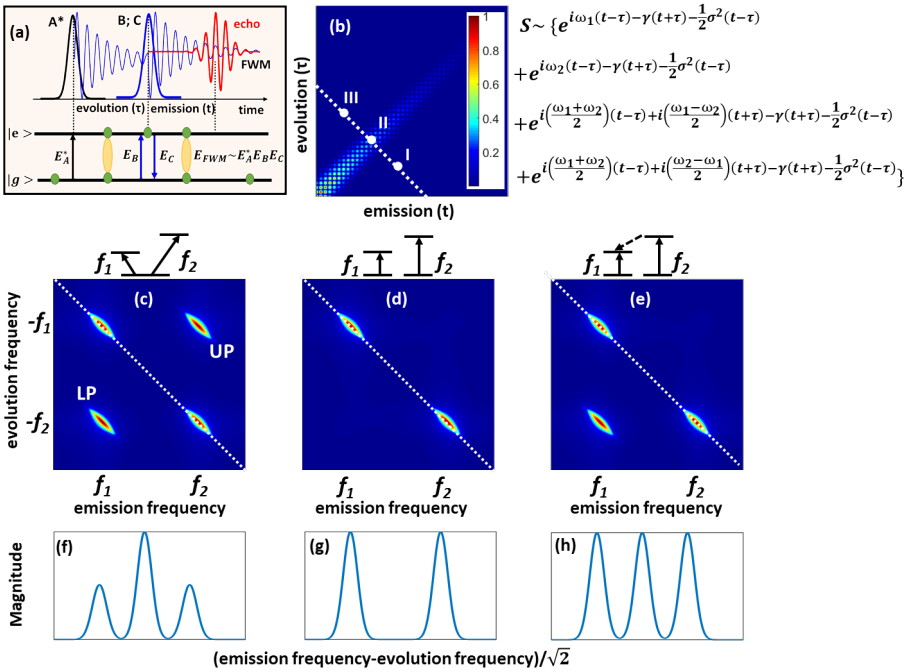

Fig. 1. (a) Photon-echo excitation scheme using a sequence of (A*-phase conjugated, B, C) pulses. Four-wave-mixing (FWM) echo signal is formed at t=τ. $|g\rangle$ and $|e\rangle$ correspond to the ground and excited states. (b) Cartoon showing the magnitude of a FWM signal as a function of evolution (τ) and emission (t) times. The equation describes a photon echo signal for a simple V-type system. ω is the transition frequency, γ is the homogeneous linewidth, σ is the inhomogeneous linewidth. The first and second terms correspond to the signals with the same ω_1 (ω_2) evolution and ω_1 (ω_2) emission frequencies (diagonal peaks in (c)), whereas the third and fourth terms correspond to the signals with ω_1 (ω_2) evolution and ω_2 (ω_1) emission frequencies (cross peaks in (c)). The dotted line on the figure shows a Fourier slice along (t-τ) which is the same as the Fourier transform of the equation with respect to (t-τ). (I), (II) and (III) points are illustrated in figure (2). (c) 2D spectrum of a V-type system. UP-upper cross peak, LP-lower cross peak. (d) 2D spectrum of two independent two-level systems.(e) 2D spectrum of a coupled 2 two-level systems. In (c), (d) and (e) the evolution frequency is negative to reflect the negative phase evolution during the evolution period shown in (a). (f), (g) and (h) Fourier transform of a slice for (c), (d) and (e) systems, respectively.

coherent spectra. This approach is based on the Fourier-slice (projection-slice) theorem [17], [18] which states that the Fourier-transform of a slice of a two-dimensional function is equivalent to a projection of the function on that axis in the Fourier domain. Graphically this point is demonstrated in figure 1 (b). The one-dimensional Fourier transform of the slice shown in figure 1 (b) is equivalent to the projections of figures 1 (c), (d), and (e) on their diagonal lines. The one-dimensional Fourier transforms of the slices for three different systems (described in this paper) are shown in figures 1 (f), (g), and (h) which are the same as the projections of their corresponding 2D spectra on the diagonal lines. These figures clearly show different patterns (compared to traditional 1D spectra) and the coupling peak is the key to differentiate these systems from each other (more details about how to differentiate figures 1 (f) and (h) are described later). We should note that, this approach was inspired by the dual-comb spectroscopy detection technique [19], [20], [21] that can allow the measurements along the slice in figure 1 (b) rapidly (simultaneously along t and τ) without using any mechanical moving parts (described below) which is obviously desirable for practical applications.

II. Experimental Setup

A simplified schematic diagram of our experimental setup is shown in figure 2 (a). We used two home-built 540 MHz repetition rate frequency combs (Ti:Sapphire lasers) centered at 800 nm. We used free-running combs since our data acquisition only takes $\sim$ 100 μs (please see below for details) and the combs' relative jitters are negligible on this time scale. The output of Comb 1 was split into two parts. One part was combined with Comb 2 and focused on the sample. The second part of Comb 1 was slightly delayed ($\sim$10 ps) and fixed with respect to the first part and used as a local oscillator to interfere on a detector with signals generated from the sample. Our combs had slightly different repetition rates ($\sim$50 Hz) which allowed Comb 2 pulses to be scanned with respect to Comb 1 (increasing τ) and simultaneously photon echo pulses to be scanned with respect to LO pulses (decreasing t) as shown in figure 2 (b). This arrangement is equivalent to scanning along the line shown in figure 1 (b). Points I, II, and III correspond to echo pulses right before, on top and right after the LO pulses, respectively. We should note that in our experiment we used co-linear excitation geometry, which is desirable for imaging applications, and linear and nonlinear contributions were separated in the RF domain. The separation of linear and echo signals are shown in figure 2 (c). The black lines (f_A = f_{LO}) correspond to Comb 1 teeth with frequencies nf_{rep_1}+f_{o_1} (n is an integer, f_{rep_1} is the repetition frequency of comb 1, f_{o_1} is the offset frequency of comb 1). The blues lines (f_B = f_C) correspond to Comb 2 teeth with frequencies m$f_{rep_2}+f_{o_2}$ (m is an integer, f_{rep_2} is the repetition frequency of comb 2, f_{o_2}

This article has been accepted for publication in IEEE Photonics Technology Letters. This is the author's version which has not been fully edited and content may change prior to final publication. Citation information: DOI 10.1109/LPT.2023.3325799

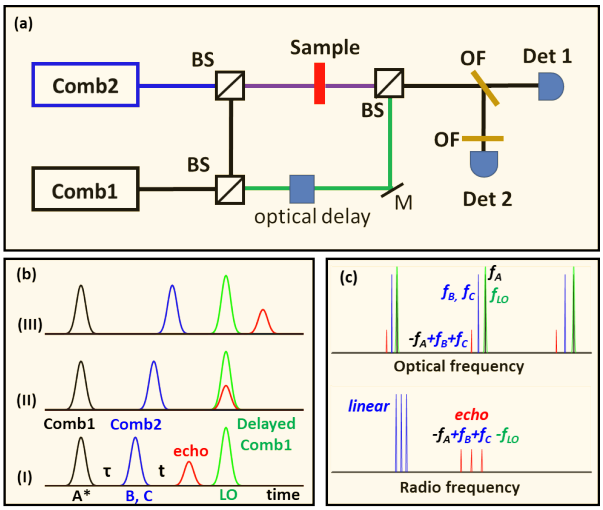

Fig. 2. (a) A simplified schematic of our experimental setup. BS-beam splitter, M-mirror, OF-optical filter, Det-Detector. (b) A cartoon showing Comb 2 pulses (blue) sweeping with respect to Comb 1 pulses (black) and generated FWM echo pulses (red) simultaneously sweeping through the LO pulses (green). (I), (II), and (III) depict different points in figure 1 (b). (c) (top) A schematic diagram showing the generation of a FWM- photon echo signal (in the optical domain) using Comb 1 and Comb 2 teeth. (c) (bottom) Separation of linear and the photon echo signals in the RF domain after interfering with the LO Comb.

is the offset frequency of comb 2). The red lines correspond to the teeth of the echo comb with $(-f_A + f_B + f_C)$ frequencies ($E_{echo} \sim E_A^* E_B E_C$). Interference (beating) of LO comb lines (green) with blue (linear) and red (echo) lines causes the spectrum to be down-converted and linear $(f_B - f_{LO})$ and echo signals $(-f_A + f_B + f_C - f_{LO})$ to be separated in the RF domain as shown in Figure 2 (c) (bottom). In our experiment, the echo signal was isolated from the linear signal using RF bandpass filters and the output of the detector was digitized using a fast data acquisition board. The data was analyzed using Matlab.

For this proof-of-concept experiment, we used rubidium atoms as our sample that is a V type system (similar to figure 1 (c)) with D1 and D2 absorption lines at 795 nm (377 THz) and 780 nm (384 THz), respectively. The sample was loaded in a cell with 1 mm length and heated up to 130 degree C. It is important to note that the projection-slice acquisition approach described above, causes UP and LP peaks (shown in figure 1 (c)) for a V type system to be projected on top of each other. This clearly would not allow one to distinguish systems shown in figure 1 (c) and (e) because for both cases the coupling peak would be present on their corresponding spectra (as shown in figure 1 (f) and (h)). To address this issue and realize a more general approach, in our experiment, we added an optical interference filter ($\sim$ 3 nm FWHM) in front of Det 1 that passes 780 nm light. The reflected portion of the beam, which contains the signal at 795 nm (780 nm light is eliminated), was simultaneously detected on Det 2. In order to completely eliminate 780 nm light, we used an optical bandpass filter (centered at 795 nm) in front of Det 2 as well. This arrangement allows UP and LP to be detected separately (please see figure 3 below for details) which is critical for sample identification. The presence of UP and LP in the measured spectra would indicate the case shown in figure 1 (c), the absence of UP would indicate the case shown in figure 1 (e), and the absence of UP and LP would indicate the case shown in figure 1 (d).

III. Results

Results of the experiment are shown in figure 3. Figure 3 (a) shows a typical linear absorption dual-comb spectrum with D1 and D2 absorption lines. This spectrum was measured separately since in our main experiment a nonlinear signal was the main target and it was isolated using RF bandpass filters, however it can be measured simultaneously if needed. On the other hand, in figures 3 (b) and (c) we show 1D Fourier transforms of FWM echo signals detected using detector 1 and detector 2, respectively. The spectrum obtained using Det 1 is equivalent to projections of bottom diagonal and upper cross peaks (see the inset for reference) on the diagonal dotted line whereas the spectrum obtained using Det 2 is equivalent to projections of upper diagonal and lower cross peaks. The dotted boxes correspond to optical bandpass filtering. The results clearly indicate that D1 and D2 lines belong to a V-type system (UP and LP peaks are both present) which was not reflected on the linear absorption spectrum (figure 3 (a)). This information in combination with linear spectra is very critical when investigating complex samples without prior knowledge of its constituent analytes. The spectral resolution for the peaks shown in figure 3 is $\sim$ 100 GHz and is dictated by the length of a single-shot interferogram (echo pulses interfering with LO pulses) which is obtained when B,C pulses are scanned between A* to LO pulses (separated by 10 ps). If higher resolution is required, one can improve it by increasing the delay between A* and LO pulses. The spectra shown in figures 3 (b) and (c) were obtained in $\sim$ 100 μs which is the time that Comb 2 pulses take to scan 10 ps (delay between A* and LO pulses shown in figure 2)). The acquisition time which equals to (repetition rate)/(repetition rate difference)*(10 ps) can be improved further by increasing the relative repetition rates between the combs. In contrast, measuring the cross-peaks (by obtaining a full 2D spectrum) using traditional MDCS methods would take several minutes. A full 2D spectrum can be obtained rapidly using Tri-Comb Spectroscopy [14] but it would still take several to tens of ms acquisition time. Additionally, TCS needs three combs and complex relative phase locking schemes (relative phase between the interferograms is critical) whereas our approach uses a single-shot interferogram and can be obtained using two free-running lasers.

We should emphasize that TCS and traditional MDCS methods are extremely powerful. They provide spectroscopic information about a sample (e.g. homogeneous linewidth, many-body effects, energy transfer dynamics etc) that is not accessible with other linear and nonlinear methods including the approach proposed in this paper. However, if the goal is to measure only the main and coupling peaks (critical for sensing applications) then Fourier-slice dual comb spectroscopy has clear advantages (it is faster and uses simpler apparatus) over these methods.

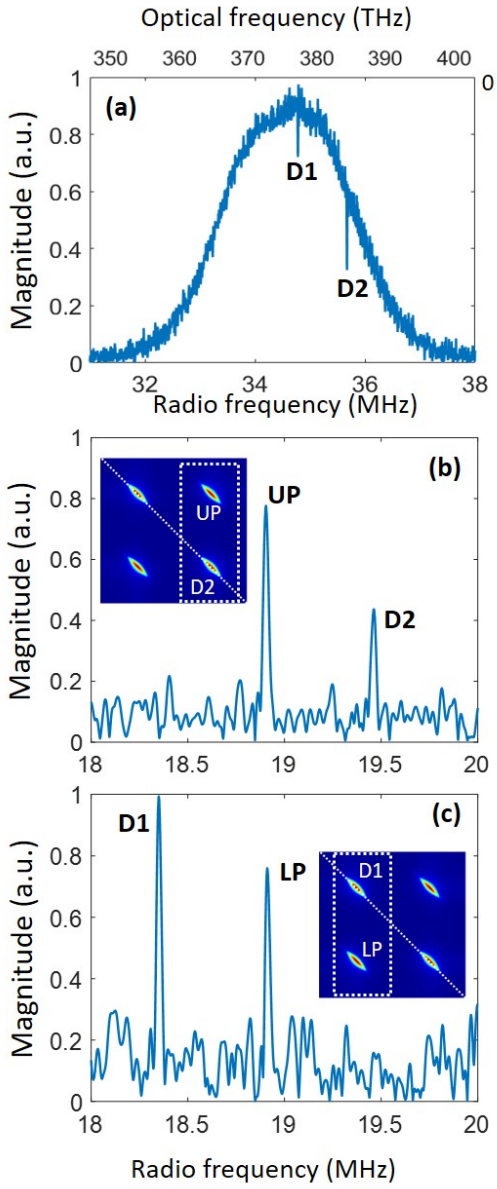

Fig. 3. (a) Linear dual-comb spectrum of rubidium D1 and D2 lines in the RF (bottom) and optical (top) domains. This spectrum was measured separately. (b) and (c) Fourier-transform of a FWM-echo signal detected on Det1 and Det2, respectively. UP and LP peaks correspond to upper cross and lower cross peaks (see insets for reference), respectively. D1 and D2 lines correspond to upper diagonal and lower diagonal peaks, respectively.

IV. Conclusion

In conclusion, we have proposed and demonstrated Fourier-slice dual-comb spectroscopy. We showed that this approach allows rapid measurements of the main absorption lines as well as the couplings between the excited states resonances which is critical for sensing applications as it addresses the issue of sample heterogeneity. This information is not easily accessible using other linear or nonlinear one-dimensional methods. Additionally, our approach uses a co-linear excitation scheme, which is desirable for imaging applications. Fourier-slice dual-comb spectroscopy can easily be combined with beam XY spatial scanning technology to obtain a two-dimensional image of a spatially heterogeneous sample rapidly with a nonlinear echo spectrum at each pixel. Additionally, with the development of compact and high power lasers (especially in the mid IR region), this method can become a field deployable for sensing applications.

Acknowledgments

The research is based on work supported by the National Science Foundation (NSF) (Grant No. 1904704). The authors thank Gary Sloan and Peter Hovland for fruitful discussions and their assistance.

References

[1] B. C. Smith, *Fundamentals of Fourier transform infrared spectroscopy*. CRC press, 2011.
[2] R. W. Boyd, *Nonlinear Optics (Third Edition)*. Burlington: Academic Press, 2008.
[3] J.-X. Cheng and X. S. Xie, *Coherent Raman scattering microscopy*. Boca Raton, FL CRC Press, 2013.
[4] T. Ideguchi, S. Holzner, B. Bernhardt, G. Guelachvili, N. Picqué, and T. W. Hänsch, "Coherent raman spectro-imaging with laser frequency combs," *Nature*, vol. 502, no. 7471, pp. 355–358, 2013.
[5] H. Li, B. Lomsadze, G. Moody, C. Smallwood, and S. Cundiff, *Optical Multidimensional Coherent Spectroscopy*. Oxford University Press, 2023.
[6] M. Cho, *Coherent multidimensional spectroscopy*, vol. 226. Springer, 2019.
[7] P. Hamm and M. Zanni, *Concepts and methods of 2D infrared spectroscopy*. Cambridge University Press, 2011.
[8] N. A. Kurnit, I. D. Abella, and S. Hartmann, "Observation of a photon echo," *Phys. Rev. Lett.*, vol. 13, pp. 567–568, Nov 1964.
[9] M. Thämer, L. De Marco, K. Ramasesha, A. Mandal, and A. Tokmakoff, "Ultrafast 2d ir spectroscopy of the excess proton in liquid water," *Science*, vol. 350, no. 6256, pp. 78–82, 2015.
[10] A. D. Bristow, D. Karaiskaj, X. Dai, T. Zhang, C. Carlsson, K. R. Hagen, R. Jimenez, and S. T. Cundiff, "A versatile ultrastable platform for optical multidimensional fourier-transform spectroscopy," *Review of Scientific Instruments*, vol. 80, no. 7, p. 073108, 2009.
[11] P. F. Tekavec, G. A. Lott, and A. H. Marcus, "Fluorescence-detected two-dimensional electronic coherence spectroscopy by acousto-optic phase modulation," *The Journal of Chemical Physics*, vol. 127, no. 21, p. 214307, 2007.
[12] E. Harel, A. F. Fidler, and G. S. Engel, "Real-time mapping of electronic structure with single-shot two-dimensional electronic spectroscopy," *Proceedings of the National Academy of Sciences*, vol. 107, no. 38, pp. 16444–16447, 2010.
[13] D. B. Turner, K. W. Stone, K. Gundogdu, and K. A. Nelson, "Invited article: The coherent optical laser beam recombination technique (colbert) spectrometer: Coherent multidimensional spectroscopy made easier," *Review of Scientific Instruments*, vol. 82, no. 8, p. 081301, 2011.
[14] B. Lomsadze, B. C. Smith, and S. T. Cundiff, "Tri-comb spectroscopy," *Nature Photonics*, vol. 12, pp. 676–680, Nov 2018.
[15] B. Lomsadze and S. T. Cundiff, "Frequency-comb based double-quantum two-dimensional spectrum identifies collective hyperfine resonances in atomic vapor induced by dipole-dipole interactions," *Phys. Rev. Lett.*, vol. 120, p. 233401, Jun 2018.
[16] B. Lomsadze and S. T. Cundiff, "Frequency combs enable rapid and high-resolution multidimensional coherent spectroscopy," *Science*, vol. 357, no. 6358, pp. 1389–1391, 2017.
[17] M. E. Siemens, G. Moody, H. Li, A. D. Bristow, and S. T. Cundiff, "Resonance lineshapes in two-dimensional fourier transform spectroscopy," *Opt. Express*, vol. 18, pp. 17699–17708, Aug 2010.
[18] G. M. Diederich, T. M. Autry, and M. E. Siemens, "Diagonal slice four-wave mixing: natural separation of coherent broadening mechanisms," *Opt. Lett.*, vol. 43, pp. 6061–6064, Dec 2018.
[19] I. Coddington, N. Newbury, and W. Swann, "Dual-comb spectroscopy," *Optica*, vol. 3, pp. 414–426, Apr 2016.
[20] I. Coddington, W. C. Swann, and N. R. Newbury, "Coherent multiheterodyne spectroscopy using stabilized optical frequency combs," *Phys. Rev. Lett.*, vol. 100, p. 013902, Jan 2008.
[21] F. Keilmann, C. Gohle, and R. Holzwarth, "Time-domain mid-infrared frequency-comb spectrometer," *Opt. Lett.*, vol. 29, pp. 1542–1544, Jul 2004.